A finite element based approach for nonlocal stress analysis for multi-phase materials and composites

Mertol Tüfekci[1,2] · John P. Dear[1] · Loïc Salles[3]

Abstract
This study proposes a numerical method for calculating the stress fields in nano-scale multi-phase/composite materials, where the classical continuum theory is inadequate due to the small-scale effects, including intermolecular spaces. The method focuses on weakly nonlocal and inhomogeneous materials and involves post-processing the local stresses obtained using a conventional finite element approach, applying the classical continuum theory to calculate the nonlocal stresses. The capabilities of this method are demonstrated through some numerical examples, namely, a two-dimensional case with a circular inclusion and some commonly used scenarios to model nanocomposites. Representative volume elements of various nanocomposites, including epoxy-based materials reinforced with fumed silica, silica (Nanopox F700), and rubber (Albipox 1000) are subjected to uniaxial tensile deformation combined with periodic boundary conditions. The local and nonlocal stress fields are computed through numerical simulations and after post-processing are compared with each other. The results acquired through the nonlocal theory exhibit a softening effect, resulting in reduced stress concentration and less of a discontinuous behaviour. This research contributes to the literature by proposing an efficient and standardised numerical method for analysing the small-scale stress distribution in small-scale multi-phase materials, providing a method for more accurate design in the nano-scale regime. This proposed method is also easy to implement in standard finite element software that employs classical continuum theory.

Keywords Three-dimensional stress analysis · Nonlocal continuum theory · Nanocomposites · Multi-phase materials · Finite element method

1 Introduction

As technology continues to evolve and devices become increasingly miniaturised, the necessity to understand the nano-scale behaviour of systems becomes more important. This is particularly crucial for applications where the precision and reliability of nano-scaled structures are essential, spanning diverse fields such as nano-robots, micro gas turbines, medical implants, security devices, and micro-electro-mechanical systems (MEMS) [1–4]. At these scales, performing experiments on material specimens becomes especially challenging due to several reasons. Firstly, it should be emphasised that meeting the extreme precision requirements for manipulating nanostructures necessitates highly specialised equipment, such as atomic force microscopes or electron microscopes, which are expensive and require specialised training to operate. Also, the behaviour of materials at the nano-scale can be significantly different from their macroscopic counterparts due to quantum effects, surface-to-volume ratio change and other scale-dependent phenomena, making it difficult to apply conventional testing methods directly. In addition, the influence of environmental factors like temperature, pressure and even molecular vibrations becomes more significant/noticeable at these scales, requiring controlled conditions that are challenging to maintain.

✉ Mertol Tüfekci
m.tufekci17@imperial.ac.uk

✉ John P. Dear
j.dear@imperial.ac.uk

Loïc Salles
l.salles@uliege.be

[1] Department of Mechanical Engineering, Imperial College London, South Kensington Campus, London SW7 2AZ, UK

[2] Centre for Engineering Research, University of Hertfordshire, College Lane Campus, Hatfield AL10 9AB, UK

[3] Department of Aerospace and Mechanical Engineering, University of Liège, 4000 Liège, Belgium

Moreover, preparing nano-scale samples that are sufficiently homogeneous for testing is itself a complex task due to the difficulties in handling and positioning nanometre-sized objects [5–7]. However, the available experimental results show that the mechanical properties such as Young's modulus are size dependent [8].

Given the numerous challenges associated with conducting experimental work at the nano-scale, the development of robust mathematical models is increasingly seen as a more practical and feasible alternative for understanding material behaviour. These models can provide accurate insights without the need for costly and complex experimental setups, making them a highly efficient tool for research in this field. Also, these mathematical models must include small-scale effects caused by lattice spaces, dislocations, grain size etc. [9, 10]. The micro/nanostructure of the materials are complex structures and behave in a complex manner; therefore, they are to be modelled using numerical tools [11–13]. Based on the literature concerning micro and nanostructure modelling, classical elastoplasticity theories generally serve as the foundational approach for material representation [14, 15]. Building upon this, classical failure theories are also commonly employed for the precise modelling of microstructure behaviour [16–18]. Nevertheless, since the rubber reinforcement and epoxy matrix interaction has to be investigated at the micro- and nano-level, the classical continuum approach would not be perfectly accurate. Instead of classical continuum theory, a nonlocal theory of elasticity seems to be a better way of modelling the elastic behaviour of the composite material [19–22]. Nonlocal continuum theory has been proposed by Ahmed Cemal Eringen and is gaining popularity in the scientific environment.

In classical continuum theory, there is no inherent length parameter that accounts for size dependencies, such as the scale of micro or nanostructures. This means that the theory assumes material properties and behaviours to be scale-independent and thus, it often fails to capture the unique characteristics observed at small scales. For instance, it doesn't consider the impacts of lattice spaces, dislocations, or grain size, which become increasingly significant at the micro and nano levels. This is the main reason why the classical elasticity theory fails to represent realistic results on such small scales. However, some studies use the classical elasticity theory and bulk material properties to model the microstructure; it is observed that they tend to keep their domain of investigations closer to the macro-scale [11, 12, 23]. Hence, when employing classical elasticity theory, the accuracy and consistency of using bulk material properties to model microstructures should be carefully considered and critically examined. This is particularly important due to the presence and characteristics of material flaws, such as dislocations and grain boundaries, which have a substantial influence at these smaller scales.

The mathematics of nonlocal elasticity is based on integral equations, as it relates the strains of all the points in the domain to the stress tensor of a point of interest. Therefore, a mathematical summation is necessary. This integral equation is analytically solvable in only some certain cases [24–30]. For instance, nanorods and nanobeams are analytically solved in many cases [31]. As of the current state of knowledge, the equations have yet to be solved analytically in three dimensions. Only numerical approximations are possible with today's knowledge [32–36].

Considering the limited cases that have analytical solutions, numerical methods are usually employed to solve such small-scale problems formulated with the nonlocal continuum theory [36, 37]. As one of the most commonly used numerical methods, the finite element method is also often preferred to construct models using the nonlocal continuum approach. Also, in the literature, the number of studies that formulate two-dimensional and three-dimensional elements is quite limited [32, 38–40]. However, there is no standardised three-dimensional numerical approach/tool formulated for nonlocal elasticity so far. The authors proposed in a previous work an approach to model nonlocal material behaviour for three-dimensional structures [38].

This theory is still being extended and developed so that it has built its own damping and failure theories [41–43]. The nonlocal theory is also being applied to nanocomposites permitting highly accurate results [44–47]. As an alternative to failure for nanocomposites, peridynamics is a popular approach which could be applied in this study as well [48–50]. The molecular dynamics approach is also one of the newest emerging approaches to nanocomposites [48, 51]. In order to understand the mechanics of materials in small-scale molecular dynamics (MD) is one of the most common ways in the modern scientific world [52]. MD simulations provide excellent and consistent insight into interactions in atomic and molecular scales. MD theory is based on the interatomic potentials defined, aiming to simulate atomic and molecular interactions. The equations that are used to perform the MD simulations require multiple parameters which are coupled directly with the expression of the empirically defined bond energies. Equations determine the accuracy of the simulations. MD simulations are performed numerically and usually, they are computationally expensive. However, they provide results that are comparable with experiments.

This study addresses the challenges in analysing small-scale multi-phase materials/composites by introducing a numerical method tailored for calculating the stress fields in nano-scale multi-phase/composite materials, with particular emphasis on weakly nonlocal and inhomogeneous materials. Hence, this research proposes an efficient and easy-to-implement and easy-to-standardise method to calculate nonlocal stresses by first calculating the local stresses

via a standard finite element method that employs classical continuum theory, which is then followed by the computation of the nonlocal stresses using the discretised version of the integral formulation of the nonlocal continuum elasticity. The novelty of this approach lies in its integration of classical finite element analysis with nonlocal continuum theory, thereby providing a straightforward transition between local and nonlocal stress calculations. Furthermore, it introduces a practical framework that is compatible with three-dimensional composites, thus enabling the incorporation of nonlocal effects into existing finite element models without a considerable increase in computational costs. This research demonstrates that postprocessing is one of the efficient and easy-to-implement/standardisable ways to calculate the nonlocal stress field. It can be easily standardised and can be applied to generic systems, such as composites or multi-phase material structures, systems with complex geometries, etc., which has not been done employing a direct finite element scheme for such complex systems yet to the best of the authors' knowledge. This research also allows one to integrate this methodology with a standard finite element tool that employs classical continuum theory, making it easy to implement and standardise. To serve as examples, a two-dimensional plate with a single circular inclusion and representative volume elements (RVEs) of various nanocomposites are generated and used. By subjecting the plate and the RVEs to a uniaxial tensile deformation, the study explores the local and nonlocal principal stress fields and their comparisons. The results obtained from the nonlocal theory reveal notable differences between local and nonlocal stress distributions, exhibiting a softening effect and mitigating stress concentrations. The methodology and results presented in this research not only propose a new numerical technique but also lay the groundwork for more precise designs and further investigations in the field, thus contributing significantly to the modelling and improvement of mechanical properties in small-scale multi-phase materials and composites.

2 Extending classical continuum theory: scale-dependent nonlocal continuum theory

Each physical theory has its domain where it is designed to work well in providing accurate predictions and descriptions of phenomena as shown in Table 1. Quantum mechanics, with its probabilistic approach, is valid at the atomic and subatomic scales, where the classical determinism of Newtonian physics fails. On the scale of molecules and nanostructures, molecular dynamics and nanomechanics represent the behaviour of systems that are still beyond the reach of macroscopic laws. As the size of the observed systems increases, the effects that dominate at the nano-scale become less pronounced and classical theories of elasticity, plasticity and the classical continuum theory begin to provide satisfactory explanations and predictions. However, these classical theories are scale-independent and assume homogeneity, which does not account for the microstructural characteristics critical at smaller scales. Nonlocal continuum theory aims to address this, introducing corrections for scale effects to classical theories, thus allowing for the analysis of phenomena where the structure and distribution of materials at the micro and nano levels play a significant role.

Table 1 Theories and fields applicable at different scales [36, 53–56]

Scale (m)	Applicable theory/field
10^{-12}	Quantum mechanics (e.g., TB, DFT, HF)
10^{-9}	Molecular dynamics, nanomechanics, nonlocal continuum theory
10^{-6}	Elasticity, plasticity, dislocation theory
10^{-3}	Mechanics of materials
10^{0}	Structural analysis

Classical continuum theory posits a scale-independent world where material properties are homogenised over infinitesimal volume elements, disregarding the actual nature of materials. Such an approach, while offering significant computational simplifications, loses fidelity when the scale of observation approaches dimensions where interatomic and intermolecular spacings are non-negligible. At these scales, the bulk properties assumption, a cornerstone of classical theory, ceases to hold true due to emergent phenomena that are inherently scale-dependent. These microscopic and nanoscopic gaps can no longer be ignored, requiring a revised theoretical framework that can accommodate the complexities of material behaviour at smaller scales. It is in this context that nonlocal continuum theory emerges, extending the classical paradigm to include the discontinuity of material structure and the consequential spatial interactions that control their mechanical responses.

2.1 Fundamental principles of nonlocal continuum theory

The classical theory of elasticity relates the stress tensor of a point to the deformation and strain tensors of the same point. It assumes the locality and claims that the stress state of a point is not affected by the deformations and strains of other points in the same continuum [23, 57–61]. However, when considering micro- or nano-scale materials, lattice spaces, atomic or intermolecular spaces become significant. In such cases, a stress tensor of a point in the continuum is affected by the deformations and strains of all other points in the

same continuum. This phenomenon is described by nonlocal continuum theory, as expressed in the following equation:

$$\sigma_{ij}^{nl}(\mathbf{x}) = \int_{\Omega} \alpha_{ijkl}\left(\mathbf{x}, \mathbf{x}', \tau\right)\varepsilon_{kl}\left(\mathbf{x}'\right)\, d\Omega \tag{1}$$

In this equation, $\boldsymbol{\varepsilon}$ denotes the strain tensor, $\boldsymbol{\sigma}$ represents the stress tensor, $\boldsymbol{\alpha}$ refers to the attenuation function, $\mathbf{x}'$ stands for the points in the domain, where the domain is shown as $\boldsymbol{\Omega}$, $\mathbf{x}$ indicates the point of interest, τ, is the nonlocal parameter that depends on the continuum and upper index "*nl*" stands for nonlocal.

It is possible to relate the characteristic lengths (the coefficients) with the stiffness, shown as $\mathbf{C}$, and/or compliance matrix.

$$\alpha_{ijkl}\left(\mathbf{x}, \mathbf{x}', \tau\right) \rightarrow \mathbf{C} \tag{2}$$

$$\sigma_{ij}^{nl}(\mathbf{x}) = \int_{\Omega} \alpha\left(\mathbf{x}, \mathbf{x}', \tau\right)C_{ijkl}\varepsilon_{kl}\left(\mathbf{x}'\right)\, d\Omega \tag{3}$$

Subsequently, the stress–strain relations of the classical theory of elasticity are incorporated into this nonlocal equation, enabling the relation between the local and nonlocal stresses to be expressed as an integral equation.

$$\sigma_{ij}^{l} = C_{ijkl}\varepsilon_{kl} \tag{4}$$

Here, the upper index "*l*" stands for local.

$$\sigma_{ij}^{nl}(\mathbf{x}) = \int_{\Omega} \alpha\left(\mathbf{x}, \mathbf{x}', \tau\right)\sigma_{ij}^{l}\left(\mathbf{x}'\right)\, d\Omega \tag{5}$$

This integral equation is analytically solvable in one and two dimensions [62, 63]. However, it becomes significantly more challenging to solve in a three-dimensional space.

2.2 The attenuation function and related parameters

Central to nonlocal continuum theory is the attenuation function, which is also known as the kernel function. This function is dependent on the distance between the field points, denoted as $\mathbf{x}'$, and the point under consideration, denoted as $\mathbf{x}$. It also considers the properties of the medium. As a result, the value of α varies across the domain of integration, reflecting the distances between points. Additionally, the configuration of the structure exerts a significant influence on this function. These structural elements are outlined as follows:

- γ: Scale factor
- e_0: Material parameter
- a: Inherent characteristic length
- l: External length scale
- τ: Nonlocal parameter

The mathematical relations between these variables are given as:

$$\gamma = e_0 a \tag{6}$$

$$\tau = \frac{\gamma}{l} = e_0\left(\frac{a}{l}\right) \tag{7}$$

The attenuation function α is bound by the following conditions:

- As τ tends to 0, α should align with a Dirac delta function. This implies the convergence of local and nonlocal elasticity theories to yield identical results for equivalent scenarios.
- Symmetry is maintained in the nonlocal tensor with respect to the field $\mathbf{x}$.
- The peak value of the nonlocal modulus occurs when $\mathbf{x} = \mathbf{x}'$ and gradually reduces to zero as the separation between the point and field points increases.
- Within an unbounded spatial domain Ω, the integral of α must equate to 1, adhering to the normalisation condition expressed as:

$$\int_{\Omega} \alpha\left(\mathbf{x}, \mathbf{x}', \tau\right)\, d\Omega = 1 \tag{8}$$

For computations within a finite volume V situated in Ω, the normalisation condition modifies as illustrated below:

$$\int_{V} \alpha\left(\mathbf{x}, \mathbf{x}', \tau\right)\, dV = 1 \tag{9}$$

Certain constants within the kernel function, like e_0, are material-specific and established, but a and l must be selected based on the structural properties. The nonlocal constants in these equations are determined with the normalisation condition in consideration.

The normalisation condition, together with the kernel function's limit as the distance extends to infinity, leads to a useful concept. One can define a radius within which the nonlocal function notably impacts the actual stresses.

For the purposes of this research, the selected attenuation function is a Gaussian function also previously used in the literature, given below and it bears the dimensions of $force * length^{-5}$ [38, 62].

$$\alpha\left(\mathbf{x}, \mathbf{x}', \tau\right) = \frac{1}{2\gamma}\mathrm{e}^{-\frac{(|\mathbf{x}-\mathbf{x}'|)^2}{l^2}} \tag{10}$$

3 Methodology and the numerical approach

3.1 Application of the nonlocal theory in discretised form

Considering the difficulties in solving the integral equation of the nonlocal continuum theory, a numerical approach is developed in this work. This approach involves discretising and solving the integral equation in Eq. 5 for three-dimensional and multi-phase materials. The discretised version of the integral equation is given as follows:

$$\sigma_{ij}^{nl}(\mathbf{x}) = \sum_{k=1}^{N} \alpha\left(\mathbf{x}, \mathbf{x}'_k, \tau\right) \sigma_{ij}^{l}\left(\mathbf{x}'_k\right) \Delta V_k \tag{11}$$

In this discretised equation, N denotes the total number of discretised points in the domain V. The domain is discretised into small volumes, each with size ΔV_k that correspond to the volume that each point represent in the discretised formulation, and the stress tensor at each point k is updated accordingly. The numerical approach allows the nonlocal stress tensor to be computed for complex three-dimensional and multi-phase materials and structures, where the analytical solution would be challenging to obtain.

The term $\alpha\left(\mathbf{x}, \mathbf{x}'_k, \tau\right)$ in Eq. 11 effectively serves as a weighting factor. This weighting captures the influence of the local stress $\sigma_{ij}^{l}(\mathbf{x}'_k)$ at a different point $\mathbf{x}'_k$ on the nonlocal stress $\sigma_{ij}^{nl}(\mathbf{x})$ at point $\mathbf{x}$. In a typical finite element model, these points $\mathbf{x}'_k$ are the values read from nodes and/or integration points in the discretised domain.

In many numerical schemes, explicit weighting factors are commonly used. However, in this model, the function $\alpha\left(\mathbf{x}, \mathbf{x}'_k, \tau\right)$ encapsulates this role. It is generally derived from the governing integral or differential equations and the boundary conditions and it may vary based on the spatial coordinates $\mathbf{x}$ and $\mathbf{x}'_k$, among other variables. As such, an additional separate weighting factor is not necessary if $\alpha\left(\mathbf{x}, \mathbf{x}'_k, \tau\right)$ is suitably defined to capture all the relevant physics and scale effects.

The proposed methodology is schematically illustrated in Fig. 1, providing a clear overview of the process for discretising and solving the nonlocal integral equation in Eq. 11.

The methodology consists of several steps. First, the domain is discretised and the local stress tensors are computed using a conventional finite element analysis software. Then, the discretised integral equation is applied to calculate the nonlocal stress tensors for each point in the domain. It is also important to note that, considering each stress components at each point of interest can be calculated independently, this approach is easy to adapt into parallel computing. Finally, the results are post-processed to obtain the nonlocal stress distributions, providing a comprehensive understanding of the stress behaviour of the studied materials. In Fig. 1, the loading is transverse, generating a stress concentration on the upper and lower surface of the inclusions. The nonlocal approach tends to smooth and remove the high stress concentration as it reduces the effect of the discontinuity.

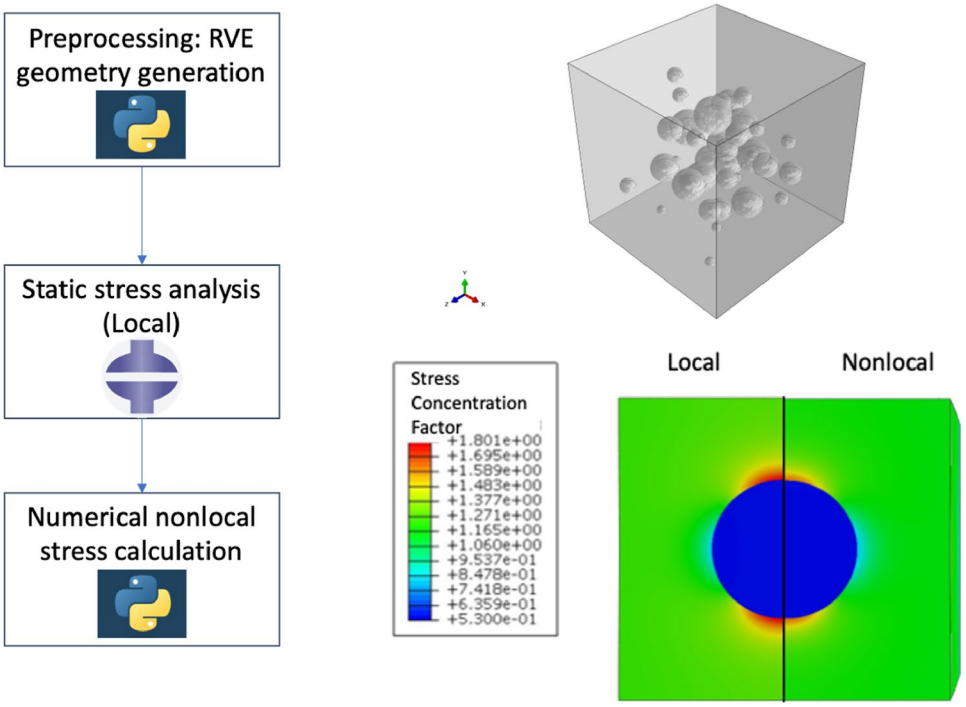

Fig. 1 Schematic view of the methodology, showing an RVE (top right) and stress concentrations on the lower and upper surfaces of the single circular inclusion in a matrix under tension for local versus nonlocal theories (bottom right)

By applying this discretised version of the integral equation to the stress analysis of three-dimensional and multi-phase materials, the nonlocal stress distributions can be obtained efficiently. This numerical approach enables investigating the stress fields of such materials with higher accuracy than the classical local continuum theory, consequently providing better understanding of the stress concentrations and overall mechanical performance. It presents a robust and efficient way to study the stress distribution and mechanical behaviour of three-dimensional and multi-phase materials exhibiting weak nonlocal characteristics. By combining local stress tensors from conventional finite element analysis with the discretised integral equation, the nonlocal stress distributions can be determined, evaluating the mechanical performance with better accuracy. Furthermore, the methodology can be easily adapted to different materials and structures, emphasising its standardisable use in the analysis and design of nano-scale, multi-phase materials and composites.

3.2 Discussion on the relationship between external length scale *l* and discretised points ΔV_k

The external length scale l plays a critical role in determining the region of integration for nonlocal stress calculations. It influences the extent to which the nonlocal effects are considered, effectively defining the interaction distance within the material. As such, the choice of l must be carefully considered in relation to the size of the discretised points ΔV_k.

The accuracy of nonlocal stress calculations depends significantly on the relationship between l and ΔV_k. If ΔV_k is too large relative to l, the discretisation may not adequately capture the nonlocal interactions, leading to inaccuracies in the computed stress fields. Conversely, if ΔV_k is too small, the computational cost may become prohibitive without a corresponding increase in accuracy.

To ensure accurate nonlocal stress calculations, it is essential to choose ΔV_k such that it appropriately resolves the scale of interactions defined by l. This often involves a balance between computational efficiency and the need for sufficient resolution to capture nonlocal effects accurately. Practical guidelines for selecting ΔV_k in relation to l include ensuring that multiple discretisation points fall within the interaction region defined by l. This typically means that ΔV_k should be an order of magnitude smaller than l to capture the gradient of the attenuation function α accurately. Hence, in this research, it is made sure that the discretisation is fine enough that the accuracy of this method.

3.3 Application of the periodic boundary conditions

To ensure periodicity in the RVEs, special attention is given to regions near the boundaries during numerical integration. In a typical scenario, the integration would be truncated at the boundary, missing contributions from neighbouring regions that could affect the stresses or strains locally. This would be mathematically expressed as:

$$\int_V f(y)\,dy \tag{12}$$

where V is the volume of the RVE and $f(y)$ represents the field variable (like stress or strain). However, truncating the integration in this way disregards the periodic nature of the system.

To address this, periodic boundary conditions (PBC) are employed to extend the integration domain across the boundaries. The program reads the corresponding points on the opposite boundaries to complete the integration, ensuring that the integrated field values reflect a periodic system. This can be expressed as:

$$\int_V f(y)\,dy = \int_V f(y+nL)\,dy \tag{13}$$

where n is an integer and L is the length of the RVE in the direction of periodicity. This equation signifies that the function $f(y)$ should be identical when shifted by any integer multiple of L, thereby satisfying periodicity.

The integrals can also be evaluated numerically using discretisation techniques. One such technique is the midpoint rule, which approximates the integral as a sum of the function values at the midpoint of discrete subintervals. For a one-dimensional function $f(y)$, the integral over a segment $[a, b]$ could be approximated as:

$$\int_a^b f(y)\,dy \approx \Delta y \sum_{i=1}^{N} f\left(a + \frac{(2i-1)\Delta y}{2}\right) \tag{14}$$

where $\Delta y = \frac{b-a}{N}$ and N is the number of subintervals.

When considering periodicity, this discretisation scheme is extended by incorporating the boundaries to form a closed loop. Hence, the periodic version of the discretised integral becomes:

$$\int_V f(y)\,dy \approx \Delta y \sum_{i=1}^{N} f\left(a + \frac{(2i-1)\Delta y}{2} + nL\right) \tag{15}$$

Here, the additional term nL ensures that when the integration reaches the boundary of the domain, it will loop back to the other end, enforcing the PBC. This approach ensures that the evaluated integral is a true representation of the field variables in a periodic system.

Boundary effects are a significant consideration in nonlocal continuum theory. The integral at the boundaries may be incomplete due to the finite nature of the domain, leading to potential inaccuracies in stress calculations near the

edges. To mitigate these effects, PBC is employed in the numerical simulations, effectively extending the domain by mirroring the values from the opposite boundaries and their neighbourhoods, thereby completing the integral even at the edges. This is shown in Fig. 2.

However, it is important to acknowledge the limitations of this approach. While PBC effectively mitigates boundary effects, it assumes that the material and structural properties are uniform across the periodic boundaries, which may not always be the case in real-world scenarios. Future improvements could involve the development of more sophisticated boundary conditions that account for non-uniform/stochastic properties and more complex geometries.

3.4 Preservation of equilibrium and conservation of angular momentum in the transformation from local to nonlocal stresses

One of the primary concerns that could be raised in the application of nonlocal continuum theory through this numerical approach is the potential violation of equilibrium conditions and conservation of angular momentum when transforming from local to nonlocal stress fields. This section addresses how this methodology maintains equilibrium and conserves angular momentum throughout this transformation, demonstrating the reliability of the nonlocal model.

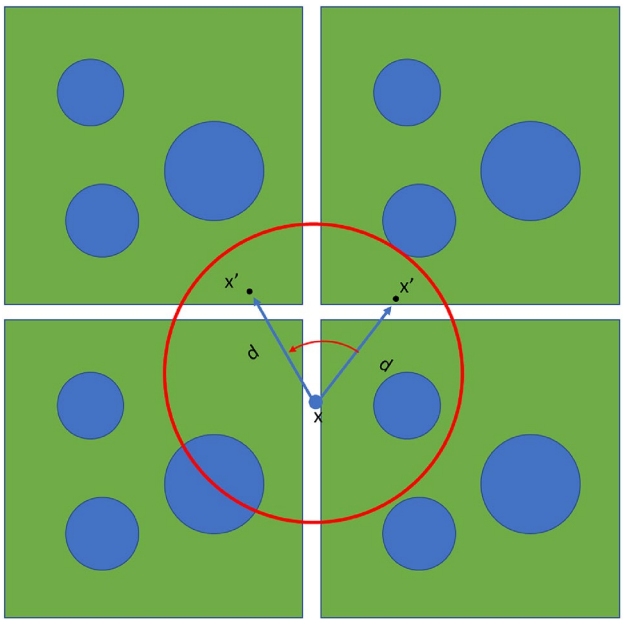

Fig. 2 A schematic visualisation of the integration procedure at the boundaries

3.4.1 Equilibrium in nonlocal continuum theory

Nonlocal continuum theory extends classical local continuum mechanics by incorporating the interactions between different points within the material as explained earlier. The primary assertion of this theory is that the stress at a point is influenced not only by the strain at that point but also by strains at different points. However, this new definition of stress, governed by the nonlocal attenuation function, does not violate the equilibrium as the transformation modifies all the stress components in a similar manner within the continuum, thus inherently preserving equilibrium. This new equilibrium can be mathematically expressed as:

$$\sigma^{nl}_{ij,i} + b_j = \rho\, \ddot{u}_j \tag{16}$$

where $\boldsymbol{\sigma}^{\mathbf{nl}}$ represents the nonlocal stress tensor, ρ stands for the material density, $\ddot{\mathbf{u}}$ indicates the acceleration of the point of interest. The divergence of the nonlocal stress tensor, $\sigma^{nl}_{ij,i}$, still sums to zero in the absence of body forces that are indicated by $\mathbf{b}$ and under static conditions where $\ddot{\mathbf{u}}$ remains as zero. This equilibrium condition has the same form as the local equilibrium condition using the local stress tensor under the classical continuum theory.

To ensure that the nonlocal continuum theory satisfies the conservation of angular momentum, it is crucial to verify that the nonlocal stress tensor remains symmetric. In classical continuum mechanics, the symmetry of the stress tensor is directly related to the conservation of angular momentum. Similarly, in nonlocal continuum mechanics, the stress tensor should be symmetric if the nonlocal interactions are properly defined.

The attenuation function α is designed to maintain the symmetry of the stress tensor. Provided that $\alpha(\mathbf{x}, \mathbf{x}', \tau) = \alpha(\mathbf{x}', \mathbf{x}, \tau)$, the nonlocal stress tensor σ^{nl}_{ij} will be symmetric, thereby satisfying the conservation of angular momentum. This condition is inherently built into the nonlocal formulation used in this study.

3.4.2 Mathematical background of equilibrium and angular momentum conservation

The transformation from local to nonlocal stresses involves an integral operator defined by the nonlocal attenuation function, α, which is a function of the Euclidean distance between material points and a characteristic length scale of the material. The nonlocal stress at a point $\mathbf{x}$ is defined as presented in Eq. 5. There, the attenuation function α is selected such that it satisfies necessary conditions like the normalisation condition described through Eq. 9 which permits the nonlocal continuum theory and its constitutive equation satisfies the thermodynamical

and conservation of momentum and energy. Hence, the construction of the nonlocal theory does not alter the overall force balance in the material. Detailed formulation and proof can be found in Chapter 6 of the book written by Eringen [59].

The conservation of angular momentum in elasticity can be expressed as:

$$\sigma_{ij} = \sigma_{ji} \tag{17}$$

This equation indicates that the stress tensor must be symmetric. In nonlocal continuum theory, the symmetry of the stress tensor is ensured through the properties of the attenuation function α.

This integral transformation adjusts each stress component to ensure the overall equilibrium for each point in the continuum is maintained. By discretising this integral equation, the numerical implementation preserves the theory's integrity without affecting the equilibrium condition, thereby ensuring that the overall equilibrium is still achieved across the continuum. The discretised form of the equilibrium equation is given by:

$$\left(\sigma^{nl}_{ij,i}\right)_k \approx 0 \tag{18}$$

where $\left(\sigma^{nl}_{ij,i}\right)_k$ represents the nonlocal stress at discretised points indicated by k. The discretised form of the equilibrium equation upholds this, demonstrating that the formulation remains consistent even in its numerical application and it does not introduce any imbalance or nonphysical forces within the system [59].

3.4.3 Verification of equilibrium and angular momentum conservation through numerical simulations

To validate the preservation of equilibrium conditions and conservation of angular momentum, numerical simulations check the balance of internal and external forces following the application of the nonlocal transformation. These simulations are structured to confirm that the approximation in Eq. 18 holds across the computational domain, ensuring that the nonlocal model does not introduce any source of imbalance or violation of angular momentum conservation.

Verification through these simulations confirms that the numerical application of nonlocal continuum theory maintains equilibrium at both local and global scales, thereby validating the integrity of the computational model in alignment with the foundational principles of continuum mechanics. Additionally, the symmetry of the nonlocal stress tensor is verified numerically to ensure conservation of angular momentum.

Table 2 Material properties for MAT 1 and MAT 4 for $L/a = 3, 10, 20$ where L is the plate dimension and a is the inclusion diameter [64]

Materials	MAT 1-local		MAT 4-nonlocal	
Material properties	Inclusion	Matrix	Inclusion	Matrix
G (GPa)	0.5	1.0	0.5	1.0
ν	0.25	0.33	0.25	0.33
ξ	1.0	1.0	ξ_{opt}	ξ_{opt}
κ/a	–	–	0.2	0.2

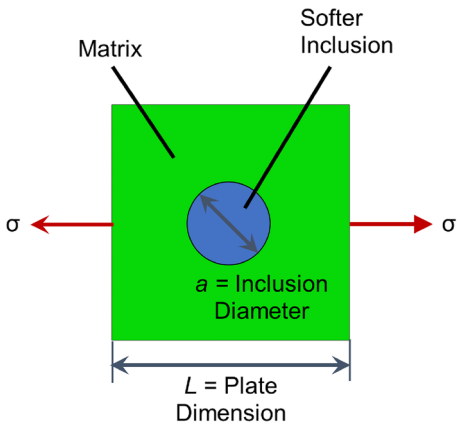

Fig. 3 A view of a generated representative element with a single circular inclusion (two-dimensional case previously analysed by Tuna et al. [64])

4 Numerical examples

4.1 Two-dimensional plate with a single circular inclusion

The first numerical example, shown in Fig. 3, is selected as a two-dimensional case which is based on a previous study by Tuna et al. [64]. The study by Tuna et al. investigates the stress fields and concentrations in a two-dimensional plate containing a single circular inclusion under uniaxial tensile loading in the transverse direction. The analysis aims to compare local and nonlocal continuum theories when modelling the size effects associated with the inclusion geometry. The plate has width L and the inclusion has radius a, with scale ratios L/a of 3, 10 and 20 examined. Linear elastic isotropic materials are defined for the matrix and inclusion phases using shear modulus G and Poisson's ratio μ. Four material configurations are studied but here, only MAT 1 and MAT 4 are studied where MAT 1 consists of a local matrix and inclusion and MAT 4 includes a nonlocal matrix and inclusion. The nonlocality is based on Eringen's nonlocal theory over the nonlocal

the parameters κ and ξ. It must be clearly stated that the research by Tuna et al. uses a different attenuation function to this study. However, it is already explained earlier that the attenuation functions must possess certain characteristics which brings them to a similar from and therefore, through a basic curve-fitting approach, the attenuation function and nonlocal parameters used in this present study are calibrated to fit the study by Tuna et al. [64]. The stress fields, stress concentration factors, convergence and nonlocal interactions are analysed. Through this numerical case study, the similarities and differences between the approach proposed in this study and the finite element model developed by Tuna et al. are compared. This analysis relates to inclusions and simulation domains with a scale of a few nanometres.

The properties for MAT 1 (local) and MAT 4 (nonlocal) are presented in Table 2.

4.2 Representative volume elements of composites with random spherical inclusions

This section explores the stress behaviours of various nanocomposites using finite element models. The numerical analyses for this investigation utilise Young's modulus values of 70 GPa for fumed silica (FS), 200 MPa for rubber (Albipox 1000), and 10 GPa for silica (Nanopox F700), aligning with the calculations performed in the study by Tüfekci et al. [65]. The representative volume elements (RVEs) of these nanocomposites are designed with PBC and are subjected to a uniaxial tensile strain of 0.01. It is worth noting that the selection of those inclusions permits exploration of the effects of the sizes of the particles as well as the relative stiffness of the inclusions compared to the matrix.

The initial step in constructing the finite element models involves generating an RVE with randomly positioned and sized reinforcement particles. These particles are carefully arranged so as not to intersect either each other or the boundaries of the RVE, as detailed in various studies [66–69]. To ensure reliable material behaviour, the side length of the cubic RVE is chosen to be at least five times the largest dimension of any particle within it [70, 71]. Figure 4 provides a visual example of a generated RVE used in this study.

After generating the RVEs, stress analyses are initially conducted using classical continuum methods. These models serve as the basis for further analysis employing the numerical approach described earlier for calculating nonlocal stresses. To achieve reliable and repeatable results, each set of material parameters is subjected to analysis five times. Finally, a comparative visualisation of the principal stresses calculated under local and nonlocal continuum theories is undertaken, shedding light on their differences and similarities.

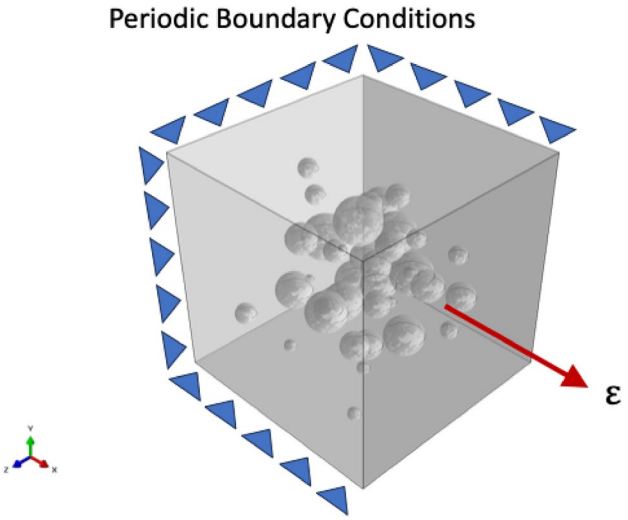

Fig. 4 A view of a generated RVE with spherical inclusions

To support and justify the usage of the nonlocal continuum theory, the sizes of the molecules, particles and RVEs are presented in Table 3. As it can be seen from the data provided, the sizes of the molecules and RVEs are relatively close which suggests that the RVE structure would not be bulk/solid and would contain intermolecular gaps. This reinforces the necessity of a more advanced and scale-dependent continuum theory when analysing these RVEs as also suggested by the data in Table 1 [36, 53–56].

It is crucial to emphasise that all the cases created with the RVEs are all individual since the reinforcement particle sizing and positioning are done randomly whilst keeping the volume fraction of the reinforcements constant at 10%. Therefore, the nonlocal parameters that are imposed on each RVE have to be different in terms of numerical values. However, the nonlocal size parameter γ is chosen for each case based on the RVEs and inclusions' geometric properties. The extrinsic length is selected as the RVE parameter and the intrinsic length is chosen as the average reinforcement diameter. The material constant e_0 is determined based on the literature [25, 75, 76]. Overall the nonlocal size parameters γ for the epoxy and rubber (Albipox 1000) come down to a range of approximately 0.08–0.13, while for FS and silica (Nanopox F700), the size parameters lie in the range of 0.15–0.21.

Table 3 The molecule and RVE sizes for the materials used for this set of examples [72–74]

Material	Basic unit dimension	Extended molecular particle dimension	Maximum RVE sizes
Epoxy Resins	~ 1.4 nm (BADGE monomer length)	Nanometres to micrometres (polymer network)	–
Albipox 1000 (CTBN Rubber)	~ 0.44 nm (butadiene), ~ 0.25 nm (acrylonitrile)	Tens to hundreds of nanometres (extended polymer chain)	5000 nm
FS and Nanopox F700 Silica (SiO_2)	~0.16 nm (Si-O)	5–50 nm (nanoparticles), indefinite in network solid	250 nm

Table 4 Comparison of stress concentration factors between Tuna et al. [64] and this study for MAT 1 and MAT 4

Materials	MAT 1-local		MAT 4-nonlocal	
L/a	Tuna et al. [64]	This study	Tuna et al. [64]	This study
3	1.78202	1.801	1.5424	1.530
10	1.68808	1.692	1.45891	1.448
20	1.6768	1.688	1.44371	1.435

5 Results of the numerical examples and discussion

5.1 Two-dimensional plate with a single circular inclusion

The results of the numerical examples are presented in Fig. 5 and Table 4 showing the stress distribution and concentration factors for a two-dimensional plate with a single circular inclusion. The findings are compared with a nonlocal analysis conducted by Tuna et al. [64]. Figure 5 illustrates the stress results through a section view of the representative element with a circular inclusion, highlighting the stress distribution patterns within the matrix.

The comparison of stress concentration factors, as summarised in Table 4, delineates the performance of both local (MAT 1) and nonlocal (MAT 4) models in terms of stress handling at various plate-to-inclusion size ratios L/a. For MAT 1, the stress concentration factors derived from this study are in close agreement with those reported by Tuna et al., with the maximum difference observed being approximately 1.07% for $L/a = 3$. This minor discrepancy underscores the precision and reliability of the methodologies employed in this investigation, despite the differences in approach.

In the context of the nonlocal model (MAT 4), which incorporates the softening effect and thus leads to a reduction in stress concentrations, the findings of this study are again in good alignment with those of Tuna et al. Particularly noteworthy is the case for $L/a = 3$, where Tuna et al. report a reduction in stress concentration factor by around 14%, a figure closely mirrored by the results of this study, which indicate a reduction of approximately 13.98%. This reduction exemplifies the efficacy of the nonlocal model in mitigating stress concentrations, attributed to its ability to account for scale effects and the long-range interactions within the material microstructure.

The stress distribution visualised in Fig. 5 further illustrates the distinction between local and nonlocal models. The nonlocal model, in alignment with classical continuum theory, exhibits a smoother stress distribution when compared to its local counterpart. This smoothing effect is indicative of the nonlocal model's capacity to more accurately reflect the physical behaviour of materials at smaller scales, where classical theories may fall short.

Subsequently, the equilibrium conditions for each node are inspected using the approach described in Sect. 3.4 and it is revealed that the equilibrium is satisfied, remaining within allowable numerical tolerances.

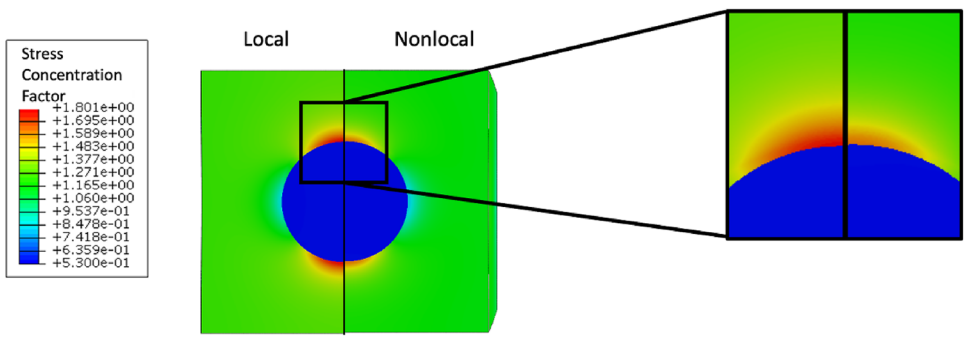

Fig. 5 The stress results through a section view of a the representative element with a circular inclusion ($L/a = 3$) under a transverse loading

5.2 Representative volume elements of composites with random spherical inclusions

The major principal stress distribution of the composite reinforced with FS is shown in Fig. 6a. It can be seen that the stress concentrations occur around the reinforcing FS particles due to caused discontinuity. Relatively uniform stress distributions are observed in the matrix away from the particles. The maximum stress in the matrix appears on the boundaries of the FS particles. The compression stresses

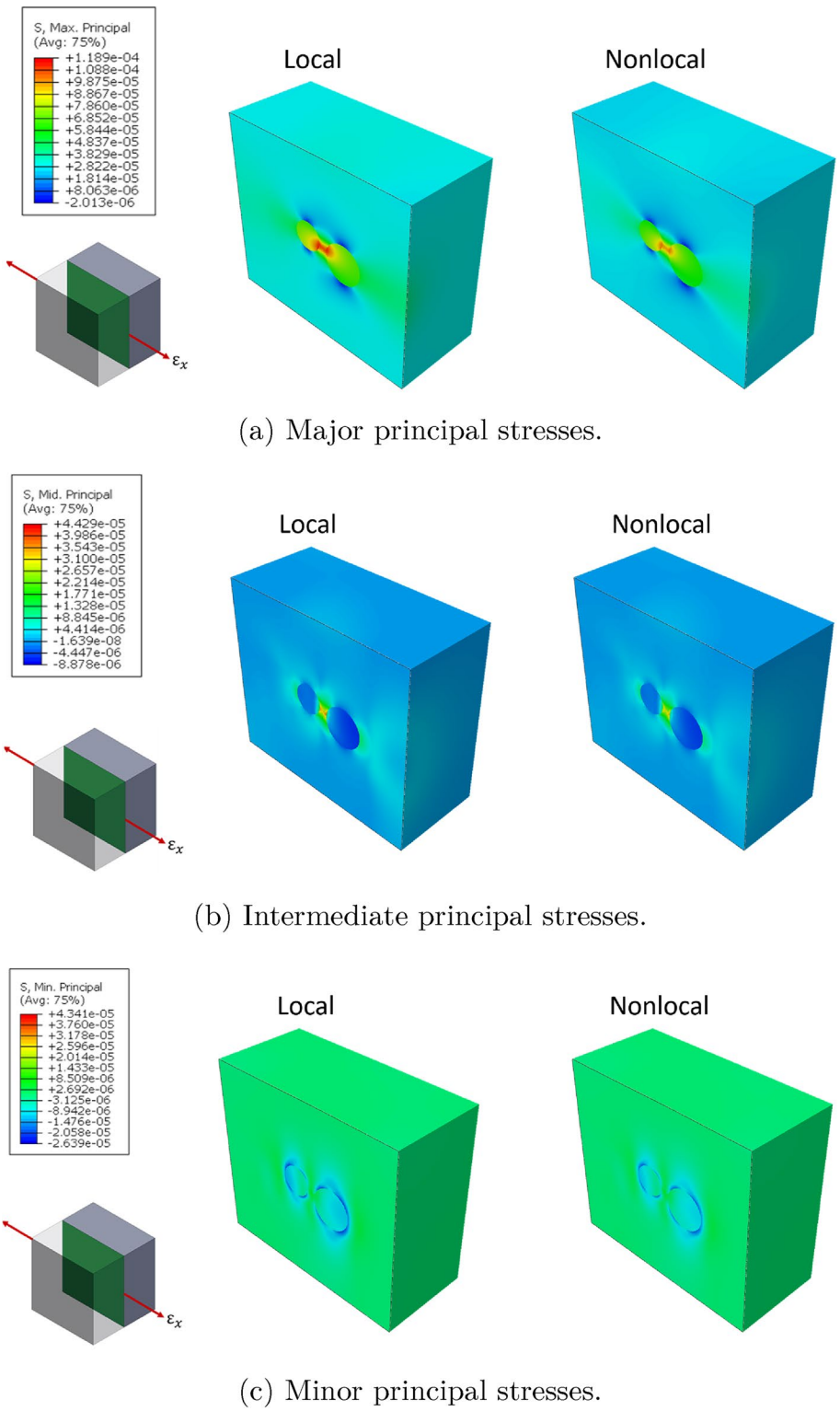

Fig. 6 Comparison of local and nonlocal continuum theories over principal stress fields (**a** major, **b** intermediate and **c** minor principal stress fields) with multiple particles of FS-reinforced epoxy. Mean inclusion diameter 12 nm assumed between 10–15 nm (stress unit: GPa)

are observed around the boundaries of the particle since the moduli of elasticity and Poisson's ratios of the matrix and particle materials are quite different. But the magnitude of the compressive stresses are much smaller compared to the tension seen around the particles and in the particles. The maximum stress values in the matrix are read near the particles and for the nonlocal model, the stresses are lower by less than 10% than those for the local model. Thus, in the model employing the nonlocal theory, the softening effect is to be seen for both the particles and the matrix material. The stress distributions of both models are almost the same, but for the local model, the stress concentrations occur on the boundaries of the particles and the matrix is greater than in the nonlocal model.

Figure 6b shows the intermediate principal stress distribution of the composite reinforced with FS. The stress concentrations, which originate due to discontinuity in the material, are visible as tension in the surroundings and particularly between the closest FS particles. The stress distributions of both models change to compression and are largely uniform in the matrix far from the particles. The maximum stress in the epoxy matrix is observed between the neighbouring particles. The stress values both in the matrix and the rubber particles are higher in the local model by approximately 5–10% compared to the nonlocal model. Thus, in the results calculated with the nonlocal theory, a softening is observed for both the inclusions and the epoxy. The trends of stress distributions of both models are almost identical with the mentioned shift and the stress concentrations are found to be less sharp.

Figure 6c displays the minor principal stress distribution of the FS-reinforced composite. Tension-form stress concentrations are found in the area near the FS particles, similar to the maximum and intermediate principal stress distributions. Further away from the particles, the stress turns into compression and becomes relatively uniform. The maximum stresses emerge in the form of tension in the epoxy matrix around particles that are close enough where their stress concentrations can interact. The stresses in the particles are compression. Similar to the other principal stress results, the difference between the local and the nonlocal stresses are approximately 5–10%. The softening of the nonlocal continua is also observed here so the greater stresses belong to the local model. Again, the stress distribution trends are quite close to each other. Only the variations in the nonlocal model are more moderate compared to the local model.

The major principal stress distribution of the epoxy-based composite reinforced with rubber is shown in Fig. 7a. It can be seen from the figure that the stress concentrations emerge around the reinforcing rubber particles. However, the rubber particles are more compliant than the epoxy matrix. Therefore, here, the maximum stress values appear in the matrix instead of the particles, unlike in other materials. The maximum stress values in the particles' neighbourhood and the overall stress distribution for the nonlocal model are lower, by approximately 10%, than the stresses calculated with the local theory. Thus, it should be pointed out that the softening effect is observed for both the particles and the matrix material in the model using the nonlocal theory. Another thing to emphasise is that with the nonlocal theory, the stress concentrations are reduced compared to the local theory. Apart from these, the stress distribution natures of both models are quite similar.

The intermediate principal stress distribution of the rubber-added epoxy is presented in Fig. 7b. Because of the discontinuities brought on by the inclusions, stress concentrations can be identified in the form of tension close to the rubber particles. Away from a particle, the stress transforms into compression and is relatively consistent throughout the matrix. The epoxy matrix bears the most stress. The maximum stress values for the local model are greater, by around 5–10%, in both the matrix and the rubber particles than in the nonlocal calculations. The softening effect is seen in both the particles and the matrix materials in nonlocal theory. The stress distributions of the two models are just about equivalent, but for the local model, the stress concentrations happen in tension on the boundaries of the particles and the matrix, whereas for the nonlocal model, the stress distribution occurs in compression and is more continuous in the matrix away from the boundaries.

Figure 7c displays the minor principal stress distribution of the rubber added epoxy. Like the intermediate principal stress distribution, stress concentrations are observed as tension near the rubber particles. The stress distribution becomes relatively uniform in the matrix far away from the particles. The maximum stress occurs in the epoxy matrix which is identified as tension. The stresses in the particles are also tension but they are much less than the stresses observed in the matrix as the particles are softer. The maximum stress values both in the matrix and the rubber particles for the local model are higher, by approximately 5–10%, in comparison to the nonlocal model. Again, the softening effect of the nonlocal theory is to be pointed out for both the particles and the matrix phases which leads to the natural conclusion of the nonlocal model showing more consistent stress distribution and weaker stress concentrations.

Figure 8a presents the major principal stress distribution of the composite reinforced with silica (Nanopox F700). The stress concentrations are observed around the reinforcing silica particles. The matrix material displays a relatively uniform stress distribution if the points of interest are far enough from the particles. Whilst the stress concentrations appear in the matrix around the particles, as is expected and seen in the cases with FS and HNT-reinforced composites. The maximum stresses are observed in the nano-silica particles and around them as tension.

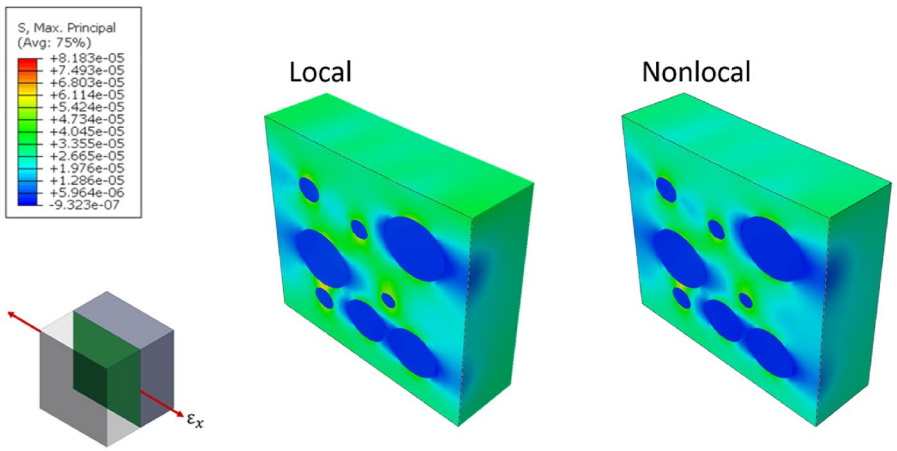

(a) Major principal stress field.

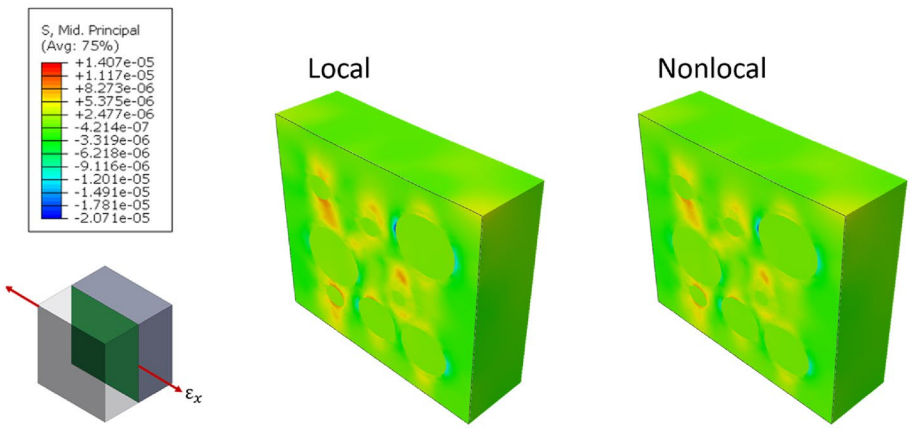

(b) Intermediate principal stress field.

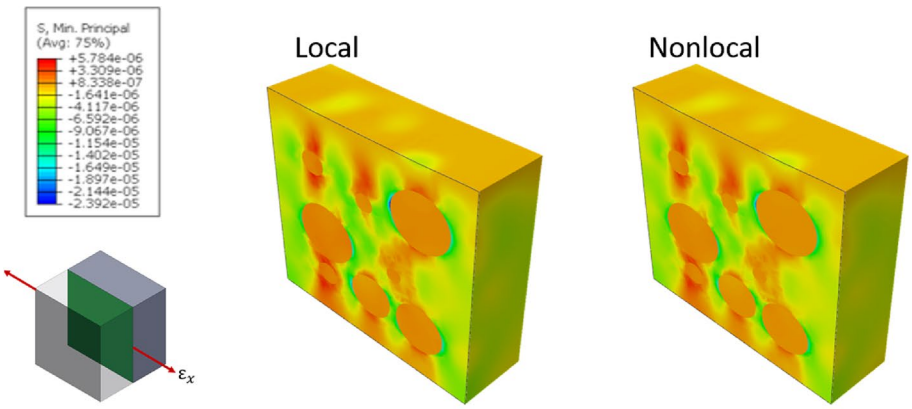

(c) Minor principal stress field.

Fig. 7 Comparison of local and nonlocal continuum theories over principal stress fields (**a** major, **b** intermediate and **c** minor principal stress fields) with multiple particles of rubber (Albipox 1000)-reinforced epoxy. Mean inclusion diameter 800 nm assumed between 500–1000 nm (stress unit: GPa)

Both models display similar characteristics in terms of the trends that the stress is distributed. But the major principal stresses at the interfaces of the particles and the matrix for the local model are roughly 10% higher than the nonlocal model, while the stress in the particles for the local model is approximately 10% higher than that calculated for the nonlocal model.

The intermediate principal stress distribution of the silica (Nanopox F700)-reinforced epoxy is shown in Fig. 8b. This time, the stress concentrations are observed

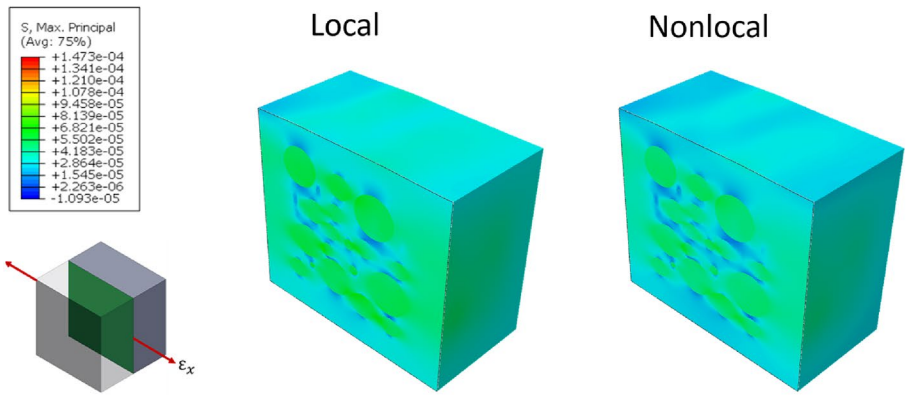

(a) Major principal stress field.

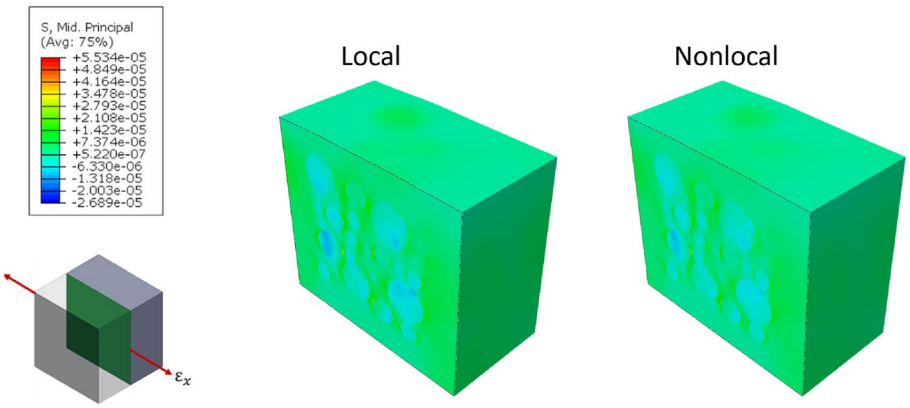

(b) Intermediate principal stress field.

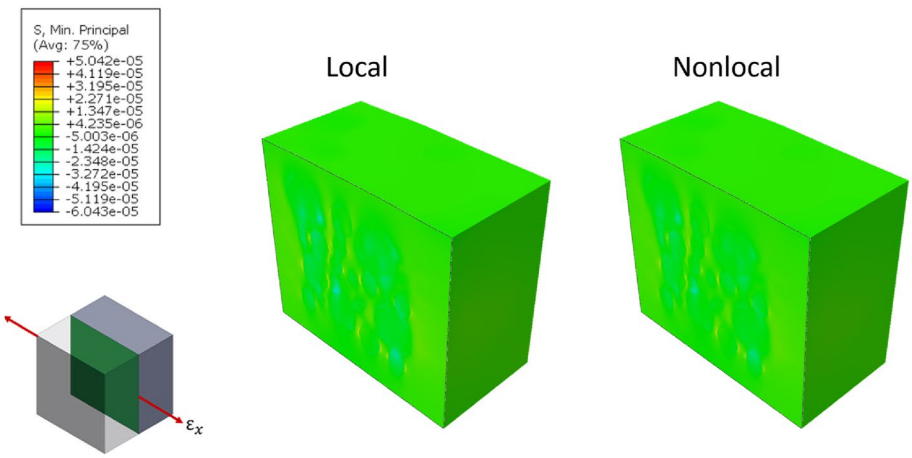

(c) Minor principal stress field.

Fig. 8 Comparison of local and nonlocal continuum theories over principal stress fields (**a** major, **b** intermediate and **c** minor principal stress fields) with multiple particles of silica (Nanopox F700)-reinforced epoxy. Mean inclusion diameter 20 nm assumed between 5–50 nm (stress unit: GPa)

as compression in the regions near the silica particles. The stress is in tension form and relatively uniform in the matrix away from any particle. The maximum stress occurs in tension in the epoxy matrix. The maximum stress values both in the matrix and the rubber particles for the local model are higher, roughly 5–10%, than those for the nonlocal model. Here, another example of the softening of the material under nonlocality is observed, which is valid for both phases, namely the matrix and the reinforcements. Other than the softening, both local and nonlocal models

exhibit similar characters in terms of the distribution of stress.

The minor principal stress distribution of the epoxy-based nanocomposite reinforced with silica (Nanopox F700) is given in Fig. 8c. The stress concentrations are observed as tension in the neighbourhood of the rubber particles, which occur due to discontinuities caused by the reinforcements, like in other cases with FS and silica reinforcements. The stress distribution changes from tension to compression and becomes more uniform in the matrix further away from the particles. The maximum stress occurs in tension in the epoxy matrix. In the particles, there are compressive stresses. The maximum stress values for the local model are roughly 5–10% higher than those computed for the nonlocal model in both the matrix and the rubber particles. The softening effect of the nonlocal theory is seen in both the particles and the matrix components of the composite. The stress distributions of the two models are nearly matching. However, for the local model, the stress concentrations are in tension at the interfaces of the particles and the matrix. whereas for the nonlocal model, the stress distribution in the matrix outside of the boundaries of the particles is in compression and is relatively uniform.

Moreover, to demonstrate the differences between the local and nonlocal models, the progressions of the maximum values of the three principal stresses during the application of strain on the RVE are illustrated in Fig. 9. The notable reduction in the slope of the stress–strain curves in the nonlocal continuum models serves as a clear indicator of a softened elastic response, compared to their local counterparts. This softening extends beyond merely lower maximum stress values; it encompasses a more even stress distribution within the RVEs, as evident by the diminished stress concentrations. Such characteristics bolster the assertion that nonlocal continuum theory provides a more faithful depiction of material behaviour under load, factoring in the scale-dependent interactions that local continuum models do not take into account.

Finally, the equilibrium conditions for each node are checked through the approach described in Sect. 3.4 and it is found that the equilibrium conditions are maintained within the acceptable numerical tolerances.

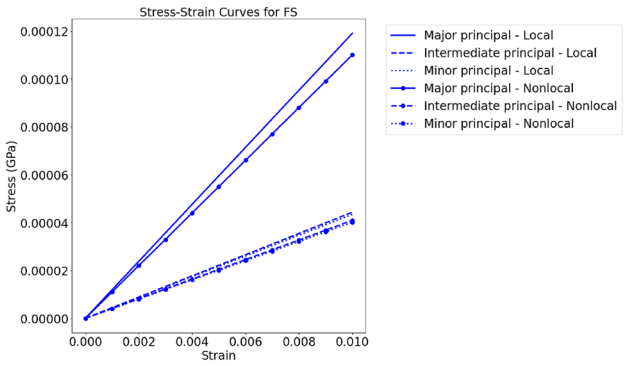

(a) FS.

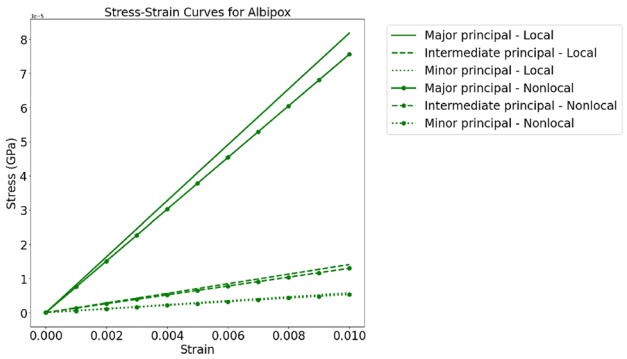

(b) Albipox 1000.

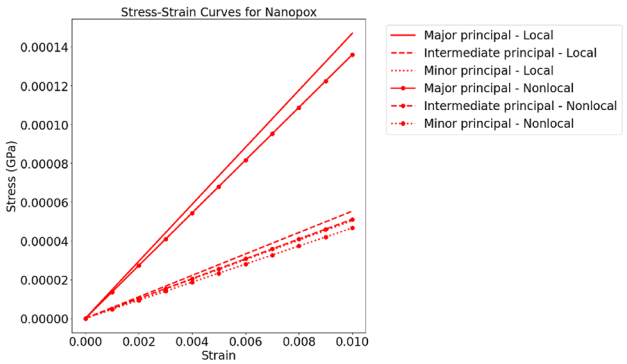

(c) Nanopox F700.

Fig. 9 Plot of the maximum of each of the three (major, intermediate and minor) principal stress versus applied strain for comparing the local and nonlocal theories **a** FS, **b** rubber (Albipox 1000) and **c** silica (Nanopox F700)

5.3 Comparison of the three-dimensional models to the literature and further discussions

Considering there is no similar work to this study in the literature, a direct/quantitative validation/comparison could not be possible. However, the nature of the results reported in the literature are found to be in good agreement with the characteristics of results of these presented numerical examples regarding the softening of the mechanical system as well as the relieved stress concentrations/reduced discontinuity [39, 40, 64, 77]. Particularly, Tuna et al. presents a comprehensive study that reveals similar behaviour as presented in Figures 6 and 7 of their study [64]. The smoothed stress distribution and the reduction of the stress concentration are clearly demonstrated, which aligns with the results of this present study. In Fig. 2 of the review by Moghtaderi et al. on the nonlocal theory shows that the nonlocal models yield lower stresses compared to the classical theories [78]. Finally Huang and Li shows that the stress concentrations

drop in composite wirh ellipsoidal inclusions as the nonlocality grows [79]. These studies, including this present study, are all qualitatively in agreement with Eringen's work who is the founder of the nonlocal continuum theory [59, 80, 81]. Eringen states that the stress concentration at a crack tip is found as infinity with the classical theory of elasticity, whereas the nonlocal continuum calculations yield finite values, which analogically indicate a reduction of the maximum stresses at a discontinuity should be the anticipated outcome. Thus, it can be claimed that this proposed method captures the physics of such weakly nonlocal nanocomposite materials with decent accuracy.

Utilising theories like the theory of mixtures and the Mori-Tanaka method for nanoparticle-reinforced composites without incorporating nonlocal theory tends to introduce inaccuracies in predicting the mechanical behaviour of these composites [65, 82–84]. These traditional approaches often employ the assumptions of the classical continuum theory and overlook the scale-dependent interactions inherent in nanocomposites and in general when small-scale mechanics are involved, leading to overstated stress predictions and, consequently, an exaggerated susceptibility to damage formation. However, when the actual stress distributions are computed using the nonlocal theory, the resultant stresses are found to be notably smaller, indicating a reduced likelihood of damage initiation under the same loads compared to the classical approach [36]. This suggests that incorporating nanoparticles as reinforcements could enhance the durability and resilience of composites more than expected.

Moreover, it is also known that using any reinforcements in a composites comes with the risk of introducing material flaws. These flaws are more significant if the size of the reinforcements are bigger [85–90]. Hence, the nanoreinforcements introduces smaller material flaws and their effects usually remain localised and limited and therefore are not as significant.

6 Conclusion

In this study, an efficient numerical approach for nonlocal stress calculation for weakly nonlocal multi-phase composites is proposed. Using this new tool, a comprehensive investigation of the stress distributions in various composites reinforced with different materials such as FS, rubber and silica is conducted. Through the application of both local and nonlocal continuum theories, the numerical simulations demonstrate distinctive characteristics of stress behaviour in the particles and surrounding matrix.

The methodology is tested on two separate cases. The first test case is a two-dimensional plate with a single circular inclusion located at the centre of the plate which is previously covered in the literature. The second test case is a collection of RVEs with randomly sized and placed spherical particles.

The nonlocal stresses, obtained by post-processing the local stresses using the discretised version of the integral equation of the nonlocal continuum theory, exhibit a notable softening effect under the same strain field. This softening leads to more moderated stress concentrations and a relatively uniform distribution away from the reinforcing particles.

Comparative analyses reveal that the stress concentrations around the particles are more significant in the local model, whereas the nonlocal model provides softer, more continuous stress distributions. In instances where materials of the matrix and the particle have significant differences in elasticity and Poisson's ratios, the nonlocal model shows a reduction in the magnitude of stress concentrations.

Furthermore, the trends in stress distributions between both models are found to be similar, but with varying degrees of stress magnitude. The nonlocal model consistently results in stress values that are approximately 5–10% lower than those for the local model, depending on the matrix and particle types.

The results suggest that calculations based on the nonlocal continuum theory provide a more accurate representation of the mechanical behaviour in nanoparticle-reinforced composites, highlighting the limitations of the classical continuum theory when small-scale mechanics are involved. This leads to a more realistic assessment of stress distributions, suggesting a reduced likelihood of damage initiation and potentially enhancing the durability and resilience of composites.

In conclusion, this study provides more understanding about the stress behaviour of composites with different reinforcements. It highlights the advantages and distinct features of applying nonlocal continuum theory, such as the mitigation of stress concentration and contributes to a more complete understanding of the interaction between matrix and particle materials with different sizes. This understanding may have significant implications for the design and application of composite materials in various engineering contexts.

Acknowledgements Mertol Tüfekci would like to acknowledge the support of Scientific and Technological Research Council of Turkey (TUBITAK), (fund BİDEB 2213 2016/2) that makes this research possible. The authors would also like to acknowledge computational resources and support provided by the Imperial College Research Computing Service (http://doi.org/10.14469/hpc/2232).

Author contributions Author statement: Mertol Tüfekci: Methodology, Formal analysis, Investigation, Software, Data curation, Writing- Original draft preparation. John P. Dear: Methodology, Writing- Reviewing and Editing, Supervision. Loic Salles: Methodology, Writing- Reviewing and Editing, Supervision.

Data availability No datasets were generated or analysed during the current study.

Declarations

Conflict of interest The authors declare that they have no known conflict of interest.

References

1. Ekinci KL (2005) Electromechanical transducers at the nanoscale: actuation and sensing of motion in nanoelectromechanical systems (NEMS). Small 1(8–9):786–797. https://doi.org/10.1002/smll.200500077
2. Koc H, Tufekci E (2023) A novel approach of bending behavior of carbon nanotubes by combining the effects of higher-order boundary conditions and coupling through doublet mechanics. Mech Adv Mater Struct. https://doi.org/10.1080/15376494.2023.2263767
3. Peddieson J, Buchanan GR, McNitt RP (2003) Application of nonlocal continuum models to nanotechnology. Int J Eng Sci 41(3–5):305–312. https://doi.org/10.1016/S0020-7225(02)00210-0
4. Di Paola M, Failla G, Pirrotta A, Sofi A, Zingales M (2013) The mechanically based non-local elasticity: an overview of main results and future challenges. Philos Trans R Soc A Math Phys Eng Sci. https://doi.org/10.1098/rsta.2012.0433
5. Rafiee R, Moghadam RM (2014) On the modeling of carbon nanotubes: a critical review. Compos B Eng 56:435–449. https://doi.org/10.1016/j.compositesb.2013.08.037
6. Geers MG, De Borst R, Brekelmans WA, Peerlings RH (1998) On the use of local strain fields for the determination of the intrinsic length scale. Journal De Physique. IV: JP 8(8):167–174. https://doi.org/10.1051/jp4:1998821
7. Bažant ZP, Pijaudier-Cabot G (1989) Measurement of characteristic length of nonlocal continuum. J Eng Mech. https://doi.org/10.1061/(asce)0733-9399(1989)115:4(755)
8. Salvetat JP, Briggs GAD, Bonard JM, Bacsa RR, Kulik AJ, Stöckli T, Burnham NA, Forró L (1999) Elastic and shear moduli of single-walled carbon nanotube ropes. Phys Rev Lett 82(5):944–947. https://doi.org/10.1103/PhysRevLett.82.944
9. Burghardt J, Brannon R, Guilkey J (2012) A nonlocal plasticity formulation for the material point method. Comput Methods Appl Mech Eng 225–228:55–64. https://doi.org/10.1016/j.cma.2012.03.007
10. Chen H, Meng C, Liu Y (2022) Modeling elasticity of cubic crystals using a novel nonlocal lattice particle method. Comput Mech 69(5):1131–1146. https://doi.org/10.1007/s00466-021-02133-y
11. Huang Y, Kinloch AJ (1992) Modelling of the toughening mechanisms in rubber-modified epoxy polymers—part I finite element analysis studies. J Mater Sci 27(10):2753–2762. https://doi.org/10.1007/BF00540702
12. Carolan D, Chong HM, Ivankovic A, Kinloch AJ, Taylor AC (2015) Co-continuous polymer systems: a numerical investigation. Comput Mater Sci 98:24–33. https://doi.org/10.1016/j.commatsci.2014.10.039
13. Zhang Y, Ren H (2023) Implicit implementation of the nonlocal operator method: an open source code, vol 39. Springer, London, pp 185–219. https://doi.org/10.1007/s00366-021-01537-x
14. Khdir YK, Kanit T, Zaïri F, Naït-Abdelaziz M (2013) Computational homogenization of elastic–plastic composites. Int J Solids Struct 50(18):2829–2835. https://doi.org/10.1016/j.ijsolstr.2013.03.019
15. Melro AR, Camanho PP, Andrade Pires FM, Pinho ST (2013) Micromechanical analysis of polymer composites reinforced by unidirectional fibres: part II-micromechanical analyses. Int J Solids Struct 50(11–12):1906–1915. https://doi.org/10.1016/j.ijsolstr.2013.02.007
16. Fish J, Yu Q (2002) Computational mechanics of fatigue and life predictions for composite materials and structures. Comput Methods Appl Mech Eng 191(43):4827–4849. https://doi.org/10.1016/S0045-7825(02)00401-2
17. Oterkus E, Diyaroglu C, De Meo D, Allegri G (2016) Fracture modes, damage tolerance and failure mitigation in marine composites. Elsevier Ltd., Amsterdam, pp 79–102. https://doi.org/10.1016/B978-1-78242-250-1.00004-1
18. Okabe T, Nishikawa M, Toyoshima H (2011) A periodic unit-cell simulation of fiber arrangement dependence on the transverse tensile failure in unidirectional carbon fiber reinforced composites. Int J Solids Struct 48(20):2948–2959. https://doi.org/10.1016/j.ijsolstr.2011.06.012
19. Buryachenko VA (2010) On the thermo-elastostatics of heterogeneous materials: I. General integral equation. Acta Mech 213(3–4):359–374. https://doi.org/10.1007/s00707-010-0282-0. arXiv:0912.4162
20. Buryachenko VA (2014) Some general representations in thermoperistatics of random structure composites. Int J Multiscale Comput Eng 12(4):331–350. https://doi.org/10.1615/IntJMultCompEng.2014010354
21. Buryachenko VA (2017) Effective properties of thermoperistatic random structure composites: some background principles. Math Mech Solids 22(6):1366–1386. https://doi.org/10.1177/1081286516632581
22. Dong H (2022) Computationally efficient higher-order three-scale method for nonlocal gradient elasticity problems of heterogeneous structures with multiple spatial scales. Appl Math Model 109:426–454. https://doi.org/10.1016/j.apm.2022.05.010
23. Eringen AC (1983) On differential equations of nonlocal elasticity and solutions of screw dislocation and surface waves. J Appl Phys 54(9):4703–4710. https://doi.org/10.1063/1.332803. arXiv:0021.8979
24. Numanoğlu HM, Ersoy H, Akgöz B, Civalek Ö (2022) A new eigenvalue problem solver for thermo-mechanical vibration of Timoshenko nanobeams by an innovative nonlocal finite element method. Math Methods Appl Sci 45:2592–2614. https://doi.org/10.1002/mma.7942
25. Civalek Ö, Uzun B, Yaylı M, Akgöz B (2020) Size-dependent transverse and longitudinal vibrations of embedded carbon and silica carbide nanotubes by nonlocal finite element method. Eur Phys J Plus. https://doi.org/10.1140/epjp/s13360-020-00385-w
26. Ömer Civalek, Uzun B, Özgür Yaylı M (2022) An effective analytical method for buckling solutions of a restrained fgm nonlocal beam. Comput Appl Math. https://doi.org/10.1007/s40314-022-01761-1
27. Albas Şeref D, Ersoy H, Akgöz B, Ömer Civalek (2021) Dynamic analysis of a fiber-reinforced composite beam under

a moving load by the ritz method. Mathematics. https://doi.org/10.3390/math9091048
28. Demir Çiğdem, Civalek Ömer (2017) On the analysis of microbeams. Int J Eng Sci 121:14–33. https://doi.org/10.1016/j.ijengsci.2017.08.016
29. Akgöz B, Civalek Ömer (2018) Vibrational characteristics of embedded microbeams lying on a two-parameter elastic foundation in thermal environment. Compos B Eng 150:68–77. https://doi.org/10.1016/j.compositesb.2018.05.049
30. Akgöz B, Ömer Civalek (2022) Buckling analysis of functionally graded tapered microbeams via Rayleigh–Ritz method. Mathematics. https://doi.org/10.3390/math10234429
31. Aydogdu M (2009) Axial vibration of the nanorods with the nonlocal continuum rod model. Phys E 41(5):861–864. https://doi.org/10.1016/j.physe.2009.01.007
32. Russillo AF, Failla G, Barretta R, Marotti de Sciarra F (2022) On the dynamics of 3D nonlocal solids. Int J Eng Sci 180:103742. https://doi.org/10.1016/j.ijengsci.2022.103742
33. Tufekci E, Aya SA (2016) A nonlocal beam model for out-of-plane static analysis of circular nanobeams. Mech Res Commun 76:11–23. https://doi.org/10.1016/j.mechrescom.2016.06.002
34. Tufekci E, Aya SA, Oldac O (2016) A unified formulation for static behavior of nonlocal curved beams. Struct Eng Mech 59(3):475–502. https://doi.org/10.12989/sem.2016.59.3.475
35. Aya SA, Tufekci E (2017) Modeling and analysis of out-of-plane behavior of curved nanobeams based on nonlocal elasticity. Compos B Eng 119:184–195. https://doi.org/10.1016/j.compositesb.2017.03.050
36. Tufekci E, Aya SA (2018) Nonlocal continuum modeling of curved nanostructures. Elsevier Inc., Amsterdam, pp 101–158. https://doi.org/10.1016/B978-0-323-48061-1.00003-8
37. Twinkle CM, Pitchaimani J (2022) A semi-analytical nonlocal elasticity model for static stability and vibration behaviour of agglomerated CNTs reinforced nano cylindrical panel under non-uniform edge loads. Appl Math Model 103:68–90. https://doi.org/10.1016/j.apm.2021.10.027
38. Tufekci M, Rendu Q, Yuan J, Dear JP, Salles L, Cherednichenko AV (2020) Stress and modal analysis of a rotating blade and the effects of nonlocality. American Society of Mechanical Engineers, pp 1–12. https://doi.org/10.1115/GT2020-14821. https://asmedigitalcollection.asme.org/GT/proceedings/GT2020/84225/Virtual, Online/1095287
39. Pisano AA, Sofi A, Fuschi P (2009) Nonlocal integral elasticity: 2D finite element based solutions. Int J Solids Struct 46(21):3836–3849. https://doi.org/10.1016/j.ijsolstr.2009.07.009
40. Pisano AA, Sofi A, Fuschi P (2009) Finite element solutions for nonhomogeneous nonlocal elastic problems. Mech Res Commun 36(7):755–761. https://doi.org/10.1016/j.mechrescom.2009.06.003
41. Nguyen TH, Bui TQ, Hirose S (2018) Smoothing gradient damage model with evolving anisotropic nonlocal interactions tailored to low-order finite elements. Comput Methods Appl Mech Eng 328:498–541. https://doi.org/10.1016/j.cma.2017.09.019
42. Sidorov V, Shitikova M, Badina E, Detina E (2023) Review of nonlocal-in-time damping models in the dynamics of structures. Axioms 12(7). https://doi.org/10.3390/axioms12070676. https://www.mdpi.com/2075-1680/12/7/676
43. Bertoldi K, Bigoni D, Drugan WJ (2007) Structural interfaces in linear elasticity. Part I: nonlocality and gradient approximations. J Mech Phys Solids 55(1):1–34. https://doi.org/10.1016/j.jmps.2006.06.004
44. Javanbakht M, Mirzakhani S, Silani M (2023) Local vs. nonlocal integral elasticity-based phase field models including surface tension and simulations of single and two variant martensitic transformations and twinning. Eng Comput 39(1):489–503. https://doi.org/10.1007/s00366-021-01598-y
45. Monetto I, Drugan WJ (2004) A micromechanics-based nonlocal constitutive equation for elastic composites containing randomly oriented spheroidal heterogeneities. J Mech Phys Solids 52(2):359–393. https://doi.org/10.1016/S0022-5096(03)00103-0
46. Drugan WJ (2003) Two exact micromechanics-based nonlocal constitutive equations for random linear elastic composite materials. J Mech Phys Solids 51(9):1745–1772. https://doi.org/10.1016/S0022-5096(03)00049-8
47. Drugan WJ, Willis JR (1996) A micromechanics-based nonlocal constitutive equation and estimates of representative volume element size for elastic composites. J Mech Phys Solids 44(4):497–524. https://doi.org/10.1016/0022-5096(96)00007-5
48. Tong Q, Li S (2016) Multiscale coupling of molecular dynamics and peridynamics. J Mech Phys Solids 95:169–187. https://doi.org/10.1016/j.jmps.2016.05.032. arXiv:0701029v1 [arXiv:physics]
49. Lu G, Chen J (2020) A new nonlocal macro–meso-scale consistent damage model for crack modeling of quasi-brittle materials. Comput Methods Appl Mech Eng 362:112802. https://doi.org/10.1016/j.cma.2019.112802
50. Candaş A, Oterkus E, İmrak CE (2023) Peridynamic simulation of dynamic fracture in functionally graded materials subjected to impact load. Eng Comput 39(1):253–267. https://doi.org/10.1007/s00366-021-01540-2
51. Paggi M, Wriggers P (2011) A nonlocal cohesive zone model for finite thickness interfaces—part II: FE implementation and application to polycrystalline materials. Comput Mater Sci 50(5):1634–1643. https://doi.org/10.1016/j.commatsci.2010.12.021
52. Srivastava D, Wei C, Cho K (2003) Nanomechanics of carbon nanotubes and composites. Appl Mech Rev 56(2):215–229. https://doi.org/10.1115/1.1538625
53. de Sciarra FM, Russo P (eds) (2018) Experimental characterization, predictive mechanical and thermal modeling of nanostructures and their polymer composites. Elsevier, Cambridge. https://doi.org/10.1016/C2016-0-00081-5
54. Steinhauser MO, Hiermaier S (2009) A review of computational methods in materials science: examples from shock-wave and polymer physics. Int J Mol Sci 10(12):5135–5216. https://doi.org/10.3390/ijms10125135
55. Shahin G, Herbold EB, Hall SA, Hurley RC (2022) Quantifying the hierarchy of structural and mechanical length scales in granular systems. Extrem Mech Lett. https://doi.org/10.1016/j.eml.2021.101590
56. Llorca J, González C, Molina-Aldareguía JM, Segurado J, Seltzer R, Sket F, Rodríguez M, Sádaba S, Muñoz R, Canal LP (2011) Multiscale modeling of composite materials: a roadmap towards virtual testing. Adv Mater 23(44):5130–5147. https://doi.org/10.1002/adma.201101683
57. Eringen AC, Suhubi ES (1964) Nonlinear theory of simple micro-elastic solids-I. Int J Eng Sci 2(2):189–203. https://doi.org/10.1016/0020-7225(64)90004-7
58. Eringen AC (1987) Theory of nonlocal elasticity and some applications. Res Mech 21(4):313–342
59. Eringen A, Wegner J (2003) Nonlocal Continuum field theories, vol 56. Springer, pp B20–B22. https://doi.org/10.1115/1.1553434. http://appliedmechanicsreviews.asmedigitalcollection.asme.org/article.aspx?articleid=1397591
60. Eringen AC (2006) Nonlocal continuum mechanics based on distributions. Int J Eng Sci 44(3–4):141–147. https://doi.org/10.1016/j.ijengsci.2005.11.002
61. Eringen AC (1967) Linear theory of micropolar viscoelasticity. Int J Eng Sci 5(2):191–204. https://doi.org/10.1016/0020-7225(67)90004-3
62. Tuna M, Kirca M (2016) Exact solution of Eringen's nonlocal integral model for vibration and buckling of Euler–Bernoulli

beam. Int J Eng Sci 107:54–67. https://doi.org/10.1016/j.ijengsci.2016.07.004
63. Barretta R, Fabbrocino F, Luciano R, Marotti de Sciarra F (2018) Closed-form solutions in stress-driven two-phase integral elasticity for bending of functionally graded nano-beams. Phys E Low Dimens Syst Nanostruct 97:13–30. https://doi.org/10.1016/j.physe.2017.09.026
64. Tuna M, Leonetti L, Trovalusci P, Kirca M (2020) 'Explicit' and 'implicit' non-local continuous descriptions for a plate with circular inclusion in tension. Meccanica 55:927–944. https://doi.org/10.1007/s11012-019-01091-3
65. Tüfekci M, Özkal B, Maharaj C, Liu H, Dear JP, Salles L (2023) Strain-rate-dependent mechanics and impact performance of epoxy-based nanocomposites. Compos Sci Technol 233:109870. https://doi.org/10.1016/j.compscitech.2022.109870
66. Pontefisso A, Zappalorto M, Quaresimin M (2015) An efficient rve formulation for the analysis of the elastic properties of spherical nanoparticle reinforced polymers. Comput Mater Sci 96:319–326. https://doi.org/10.1016/j.commatsci.2014.09.030
67. Singh IV, Shedbale AS, Mishra BK (2016) Material property evaluation of particle reinforced composites using finite element approach. J Compos Mater 50:2757–2771. https://doi.org/10.1177/0021998315612539
68. Pucha RV, Worthy J (2014) Representative volume element-based design and analysis tools for composite materials with nanofillers. J Compos Mater 48:2117–2129. https://doi.org/10.1177/0021998313494916
69. Fidelus JD, Wiesel E, Gojny FH, Schulte K, Wagner HD (2005) Thermo-mechanical properties of randomly oriented carbon/epoxy nanocomposites. Compos A Appl Sci Manuf 36:1555–1561. https://doi.org/10.1016/j.compositesa.2005.02.006
70. Gitman IM, Askes H, Sluys LJ (2007) Representative volume: existence and size determination. Eng Fract Mech 74:2518–2534. https://doi.org/10.1016/j.engfracmech.2006.12.021
71. Catalanotti G (2016) On the generation of rve-based models of composites reinforced with long fibres or spherical particles. Compos Struct 138:84–95. https://doi.org/10.1016/j.compstruct.2015.11.039
72. Jin FL, Li X, Park SJ (2015) Synthesis and application of epoxy resins: a review. J Ind Eng Chem 29:1–11. https://doi.org/10.1016/j.jiec.2015.03.026
73. Yang Z, Peng H, Wang W, Liu T (2010) Crystallization behavior of poly(ϵ-caprolactone)/layered double hydroxide nanocomposites. J Appl Polym Sci 116(5):2658–2667. https://doi.org/10.1002/app
74. Zhuravlev LT (2000) The surface chemistry of amorphous silica. Zhuravlev model. Colloids Surf A 173(1–3):1–38. https://doi.org/10.1016/S0927-7757(00)00556-2
75. Ghosh S, Kumar A, Sundararaghavan V, Waas AM (2013) Non-local modeling of epoxy using an atomistically-informed kernel. Int J Solids Struct 50(19):2837–2845. https://doi.org/10.1016/j.ijsolstr.2013.04.025
76. Karapiperis K, Ortiz M, Andrade JE (2021) Data-Driven nonlocal mechanics: discovering the internal length scales of materials. Comput Methods Appl Mech Eng 386:114039. https://doi.org/10.1016/j.cma.2021.114039
77. Kuvyrkin G, Savelyeva I, Sokolov A (2021) Solution of two-dimensional problems of nonlocal elasticity theory by the finite element method. IOP Conf Ser Mater Sci Eng 1191:012014. https://doi.org/10.1088/1757-899x/1191/1/012014
78. Moghtaderi SH, Jedi A, Ariffin AK (2023) A review on nonlocal theories in fatigue assessment of solids. Materials. https://doi.org/10.3390/ma16020831
79. Huang M, Li Z (2005) Size effects on stress concentration induced by a prolate ellipsoidal particle and void nucleation mechanism. Int J Plast 21(8):1568–1590. https://doi.org/10.1016/j.ijplas.2004.07.006
80. Eringen AC (1992) Vistas of nonlocal continuum physics. Int J Eng Sci 30(10):1551–1565. https://doi.org/10.1016/0020-7225(92)90165-D
81. Cemal Eringen A, Kim BS (1974) Stress concentration at the tip of crack. Mech Res Commun 1(4):233–237. https://doi.org/10.1016/0093-6413(74)90070-6
82. Mehdi M, Bhagat AR, Selokar GR (2018) Evaluation of effective elastic moduli using micromechanics. IOP Conf Ser Mater Sci Eng 455(1):90. https://doi.org/10.1088/1757-899X/455/1/012116
83. Luo JJ, Daniel IM (2003) Characterization and modeling of mechanical behavior of polymer/clay nanocomposites. Compos Sci Technol 63(11):1607–1616. https://doi.org/10.1016/S0266-3538(03)00060-5
84. Bisoi A, Tüfekci M, Öztekin V, Denimal Goy E, Salles L (2023) Experimental investigation of mechanical properties of additively manufactured fibre-reinforced composite structures for robotic applications. Appl Compo Mater. https://doi.org/10.1007/s10443-023-10179-9
85. Summerscales J, Dissanayake NP, Virk AS, Hall W (2010) A review of bast fibres and their composites. Part 1—fibres as reinforcements. Compos A Appl Sci Manuf 41(10):1329–1335. https://doi.org/10.1016/j.compositesa.2010.06.001
86. Summerscales J, Dissanayake N, Virk A, Hall W (2010) A review of bast fibres and their composites. Part 2—composites. Compos A Appl Sci Manuf 41(10):1336–1344. https://doi.org/10.1016/j.compositesa.2010.05.020
87. Summerscales J, Virk A, Hall W (2013) A review of bast fibres and their composites: part 3—modelling. Compos A Appl Sci Manuf 44(1):132–139. https://doi.org/10.1016/j.compositesa.2012.08.018
88. Daliri A, Zhang J, Wang CH (2016) Hybrid polymer composites for high strain rate applications. Elsevier Ltd, Amsterdam, pp 121–163. https://doi.org/10.1016/B978-1-78242-325-6.00006-2
89. Shan L, Tan CY, Shen X, Ramesh S, Zarei MS, Kolahchi R, Hajmohammad MH (2023) The effects of nano-additives on the mechanical, impact, vibration, and buckling/post-buckling properties of composites: a review. J Market Res 24:7570–7598. https://doi.org/10.1016/j.jmrt.2023.04.267
90. Liu J, Huang X, Zhao K, Zhu Z, Zhu X, An L (2019) Effect of reinforcement particle size on quasistatic and dynamic mechanical properties of Al-Al2O3 composites. J Alloy Compd 797:1367–1371. https://doi.org/10.1016/j.jallcom.2019.05.080